Korean J. Chem. Eng., **24**(2), 305-310 (2007)

Deposit morphology on SiC fibers in methane-acetylene/air laminar diffusion flames

Yu Wang and Qiang Yao†

Key Laboratory for Thermal Science and Power Engineering, Ministry of Education of China,
Tsinghua University, Beijing, 100084, China
(*Received 22 August 2006 • accepted 9 October 2006*)

Abstract–The morphologies of soot deposit on 15 μm diameter silicon carbide (SiC) fibers have been investigated with a scanning electron microscope (SEM) in methane-acetylene/air laminar diffusion flames with co-flowing air. The morphologies are shown to be strongly dependent on the fuels ratio. Two kinds of processes by which mature soot particles are produced were proved to exist in a sooting flame: one is the transition from the condensed-phase deposits; the other is the aggregation of the smaller soot particles (or chains of them) carried along the particle path line. Different transition processes are compared between the present work and previous work done by other researchers that used propane/air laminar diffusion flames. It seems the presence of C=C in methane-acetylene laminar diffusion flames is the key factor that causes the difference of transition processes in those two kinds of flames.

Key words: Deposit Morphology, Diffusion Flame, Soot, SiC Fiber, Particle

INTRODUCTION

Earlier studies of soot deposit morphologies on SiC fibers in propane/air laminar diffusion flames were done by Shim et al. [1,2]. They concluded that the average size of the mature soot deposited in the flame is strongly dependent on position in sooting flames. The transition to soot from the agglomerated condensed-phase deposits was observed in the radial direction in sooting flames. Two kinds of processes in which mature soot particles were produced existed in the flames: one was the transition from the condensed-phase deposits, while the other was the aggregation of the smaller soot particles carried along the particle path line. The fiber-like deposits, which are about 10 nm thick, were found outside the luminous flame surface and were thought to be made under the high temperature oxidation environment.

Soot particle formation (which includes nucleation, growth and oxidation) and deposition have been investigated and reviewed in numerous studies [3-13]. Saito et al. [7] studied soot morphologies of various fuels with a scanning electron microscope, using a 0.4 mm diameter quartz needle, and described the transition morphologies shown in SEM [7]. There are many studies on soot formation in hydrocarbon flames in different configurations. Two excellent reviews have been published [6,14]. The mechanism proposed by Frenklach et al. [15] in describing the chemical history of formation of a soot nucleus is widely accepted. The general idea is that the formation of a phenyl radical is the critical step to building soot by pyrolysis of the initial fuel. Acetylene molecules add to the phenyl radical with hydrogen elimination involved in each acetylene addition, thus continuing the positive buildup of mass. In the buildup process, polycyclic aromatic hydrocarbons (PAHs) are formed, finally growing large enough to be young soot particles. The earliest particles may have diameters of about 2 nm [14]. They grow by coagulation and by surface growth through reaction with gas-phase species. The thin filament pyrometry technique using SiC filament, which was developed by Vilimpoc et al. [1], has been applied in several studies for measuring the temperature profiles of non-sooting flames and soot deposit morphologies in sooting flames [1,2,16]. It has being used for its excellent spatial resolution and temporal response, because SiC fibers have sufficient temperature resistance, low thermal conductivity (11.6 J/m s K) and their surfaces do not catalyze combustion [1]. Thin SiC fibers inserted for deposition of soot scarcely disturb the flame. Therefore, they are suitable for sampling. In addition, the position of deposits in the flame can be correctly shown in SEM photographs. In the present work, SiC filaments were used to collect the deposits in methane-acetylene lami-

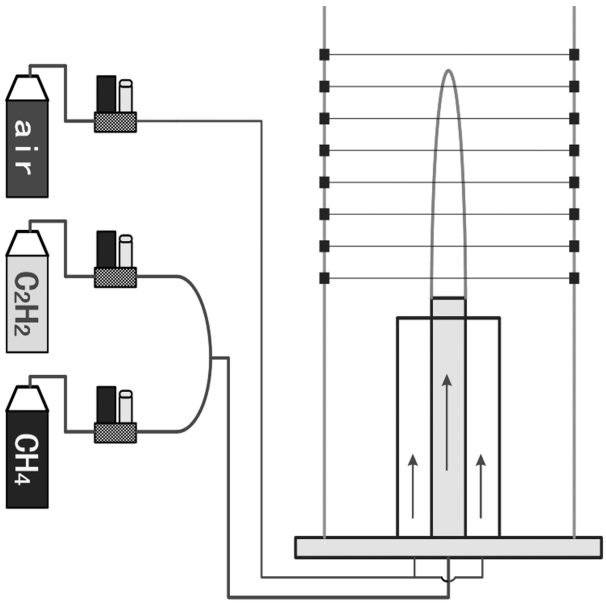

Fig. 1. A schematic of the experimental setup.

†To whom correspondence should be addressed.
E-mail: yaoq@tsinghua.edu.cn
‡This paper was presented at the 6th Korea-China Workshop on Clean Energy Technology held at Busan, Korea, July 4-7, 2006

nar diffusion flames with variation of fuel ratios in co-flowing air. All the deposits were analyzed by SEM and the results were compared with the previous outstanding studies done by Shim et al. [1,2].

EXPERIMENTAL

A schematic of the experimental set up is shown in Fig. 1 and the corresponding photograph is shown in Fig. 2. The apparatus consisted of a co-flowing burner made of quartz and mass flow controllers. The burner had an inner fuel nozzle with 10 mm inner diameter and 12 mm outer diameter. The outer tube had 32 mm inner diameter and 34 mm outer diameter through which co-flowing air was supplied. The fuel was a mixture of methane and acetylene in four different ratios which were shown in Table 1, and Eqs. (1) and (2) give the mechanism of methane and acetylene combust in air, respectively.

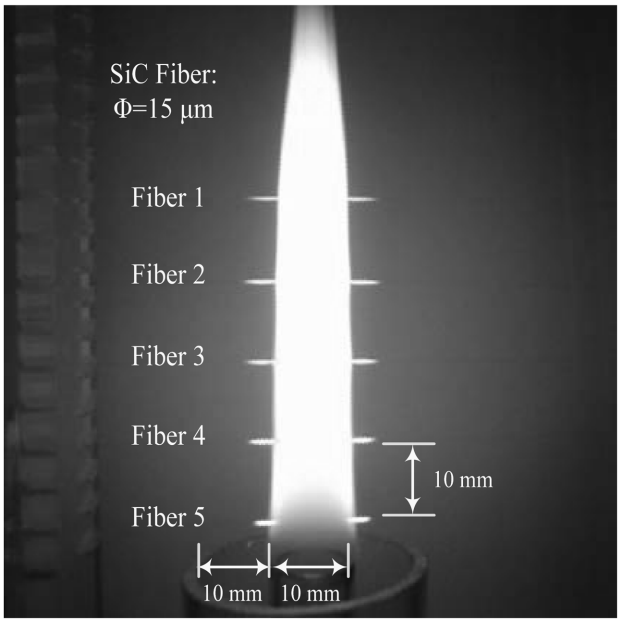

Fig. 2. A photograph of the experimental setup.

$$CH_4+2(3.76N_2+O_2)\rightarrow CO_2+2H_2O+7.52N_2 \quad (1)$$

$$2C_2H_2+5(3.76N_2+O_2)\rightarrow 4CO_2+2H_2O+18.8N_2 \quad (2)$$

15 μm diameter SiC fibers from Dow Corning were used as sites for deposits of soot. Five SiC fibers were spaced 10 mm apart with weighted free ends and were positioned horizontally across the radial centerline of the flame, each of them was about 100 mm long. These samples were analyzed with a Field Emission Scanning Electron Microscope (HITACHI S-4500, Resolution: 1.5 nm at 15 kV, Magnification: 20-200,000). They were investigated along the axial direction and radial direction of the flames. Since the deposit morphology was independent of the sampling time reported by Saito et al. [7], 2 min was chosen to be the sampling time.

RESULTS AND DISCUSSIONS

1. Case 1

Fig. 3 shows deposits on SiC fibers captured 2 min in a meth-

Table 1. Fuel and oxidizer

	Methane L/min	Acetylene L/min	Air L/min	Q/Q_{sto}
Case 1	0.25	0.00	4.7	2.0
Case 2	0.24	0.01	4.8	2.0
Case 3	0.15	0.10	5.3	2.0
Case 4	0.00	0.25	6.0	2.0

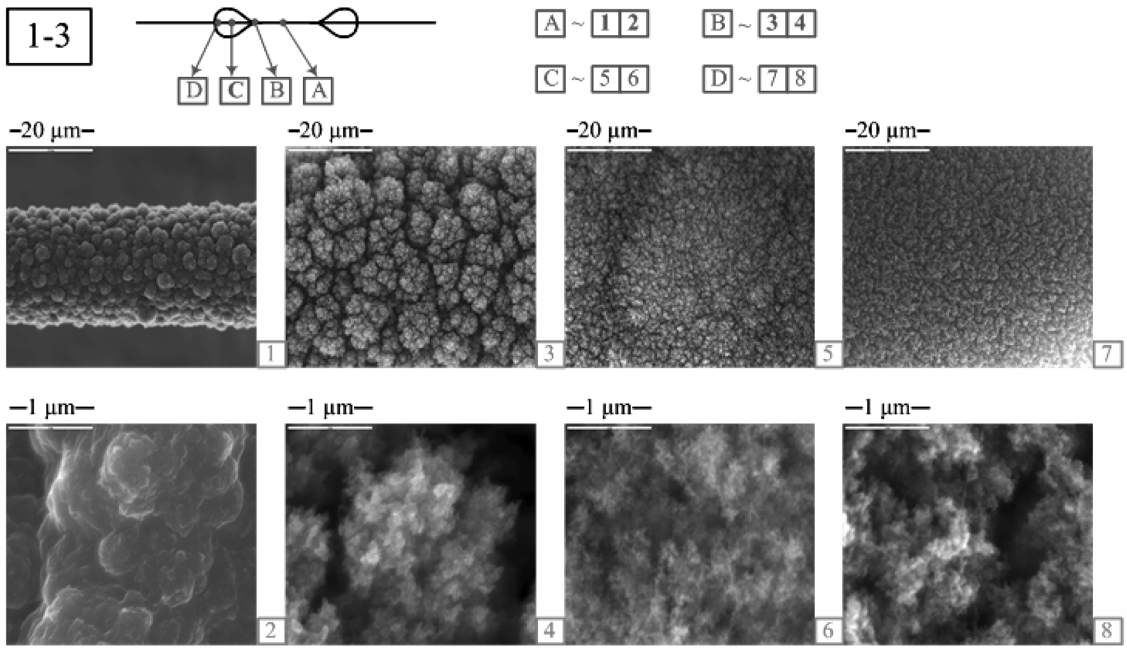

Fig. 3. Soot photographed at 2,000× (1-4) and 40,000× (5-8) by SEM. Sampled at the radial positions A, B, C and D in a methane-acetylene/air laminar diffusion flame. Nozzle ID=10 mm, Q_{fuel}=0.25 L/min with Q_{CH_4}=0.25 L/min and $Q_{C_2H_2}$=0, Q/Q_{sto}=2. Axial position: y=25 mm. The contour on the horizontal line represents deposits on the fiber.

ane-acetylene laminar diffusion flame surrounded by co-flowing air. The fuel flow rate was 0.25 L/min with 0.25 L/min methane and no acetylene. The co-flowing air flow rate was $Q/Q_{sto}=2$. "1-3" in the figure represents the third fiber from top in case 1.

The deposits on the inner region of the luminous flame at axial position y=25 mm from the burner nozzle were analyzed with SEM and shown in Fig. 3; the samples were photographed at 2,000× and 40,000× magnification. The transition from droplet-like deposits to soot particles can be seen in the photographs at 40,000×. Consistent with Shim's [1] results: the deposits first form small knobs on the largely conglomerated droplet-like surface, and the knobs grow more distinct at each step, as shown in pictures 3, 5 and 7 of Fig. 3. The lumps are broken into smaller lumps and the developed knobs begin to have the morphology of soot particles at position B. The transition occurs in a region of about 1 mm adjacent to the flame surface. The deposits at position A in Fig. 3 have about 1 μm size and have liquid-like smooth surface. The sizes of these deposits are much larger than those of the mature soot particles. As reported by Shim et al. [1,2], these large agglomerated droplet-like deposits, which are thought to be condensed-phase soot precursors, exist on the whole SiC fiber from the point studied to the opposite symmetric position in the flame. In the whole deposit region, the morphology is divided into three parts along the radial direction of the flame: (A) Around position A, a central part containing the condensed-phase large droplet-like deposits, (B) Around position B, an outer part that transition to particles from the droplet-like deposits, (C) Around position C and D, a luminous flame surface in which mature soot particles are formed and each morphology appears when the materials reach the specific corresponding positions. While the difference is that Shim used propane as fuel and $Q/Q_{sto}=13.3$ [1,2]. In Case 1 we used methane as fuel and $Q/Q_{sto}=2$. Besides, Saito et al. [7] did not find the droplet-like deposits using the quartz probe. The fuel difference will induce a morphology difference which will be discussed later in detail.

The deposit morphologies at the higher axial position of y=35 mm are different from the position of y=25 mm as shown in Fig. 4. As illustrated in the photographs at 2,000× and 40,000× of Fig. 4, the morphology of transition is similar to the previous sample, but there are no droplet-like deposits any more. Particles with a size of about 300 nm occur at position A, while the mature soot particles are about 10 nm and there is not a remarkable change between Fig. 3 and Fig. 4.

2. Case 2

Fig. 5 shows deposits on SiC fibers captured 2 min in a methane-acetylene/air laminar diffusion flame surrounded by co-flowing air. The fuel flow rate was also 0.25 L/min but with 0.24 L/min methane and 0.01 L/min acetylene, respectively. The co-flowing air flow rate was $Q/Q_{sto}=2$. "2-3" in the figure represents the third fiber from the top in case 2.

Compared with Fig. 3, the same transition from droplet-like deposits to soot particles can also be seen. But in picture 2 of Fig. 5, the droplet-like deposits are more like particles than deposits in picture 2 of Fig. 3, and particles in picture 4 of Fig. 5 are much larger than the particles in picture 4 of Fig. 3. That is, when acetylene is added into the fuel, it becomes easier to form particles, and particles grow faster than the case without acetylene. The same part is that the mature soot particles become smaller by oxidation toward the radial end of the high temperature reaction zone as shown both in Figs. 3, 4 and 5, respectively.

Fig. 6 shows the deposit morphologies at the lower axial position of y=15 mm. As in Fig. 4, there are no droplet-like deposits on the fiber, and particles sizes are all similar within 20-50 nm at positions A, B, C and D.

From Fig. 3 to Fig. 5, one process by which mature soot parti-

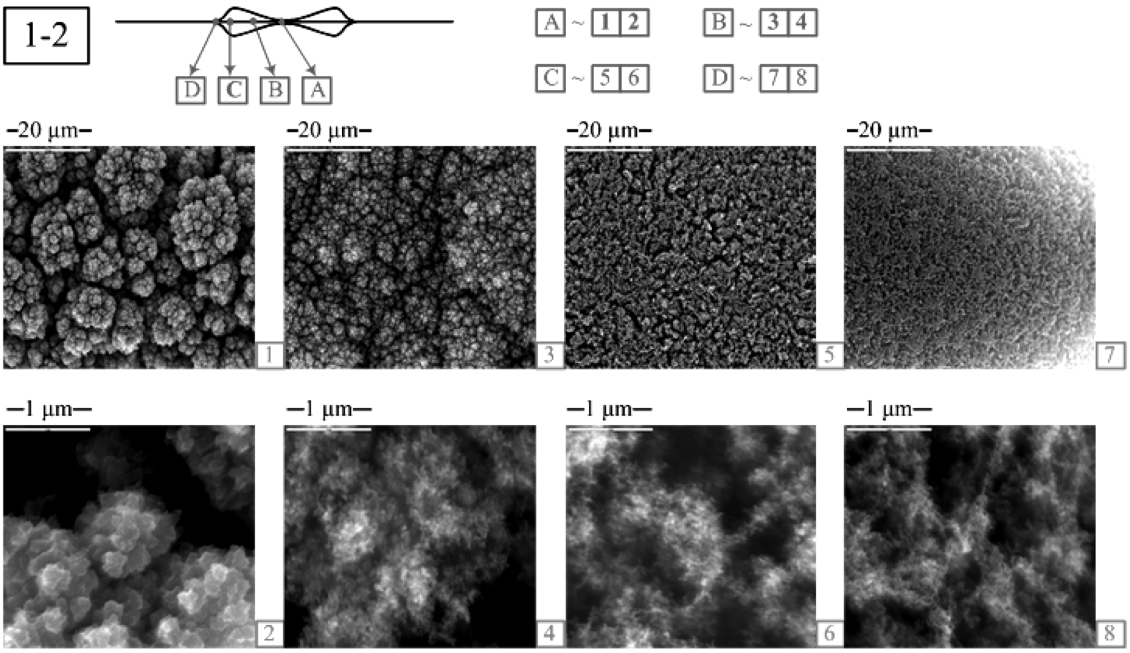

Fig. 4. Soot photographed at 2,000× (1-4) and 40,000× (5-8) by SEM. Sampled at the radial positions A, B, C and D in a methane-acetylene/air laminar diffusion flame. Nozzle ID=10 mm, $Q_{fuel}=0.25$ L/min with $Q_{CH_4}=0.25$ L/min and $Q_{C_2H_2}=0$, $Q/Q_{sto}=2$. Axial position: y=35 mm. The contour on the horizontal line represents deposits on the fiber.

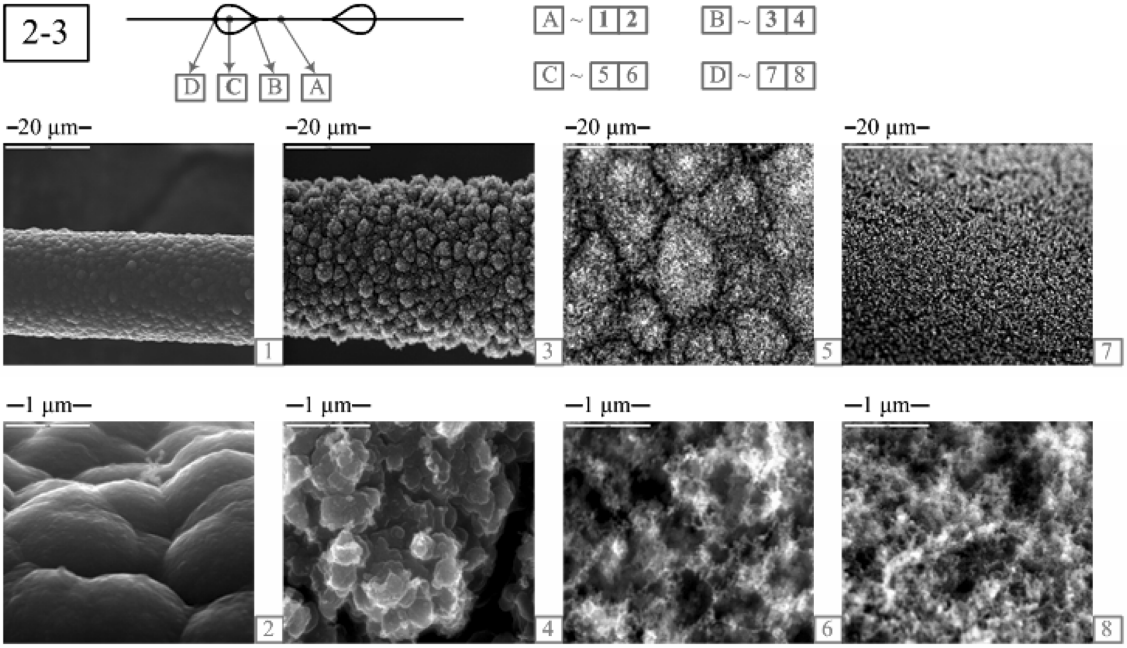

Fig. 5. Soot photographed at 2,000× (1-4) and 40,000× (5-8) by SEM. Sampled at the radial positions A, B, C and D in a methane-acetylene/air laminar diffusion flame. Nozzle ID=10 mm, Q_{fuel}=0.25 L/min with Q_{CH_4}=0.24 L/min and $Q_{C_2H_2}$=0.01 L/min, Q/Q_{sto}=2. Axial position: y=25 mm. The contour on the horizontal line represents deposits on the fiber.

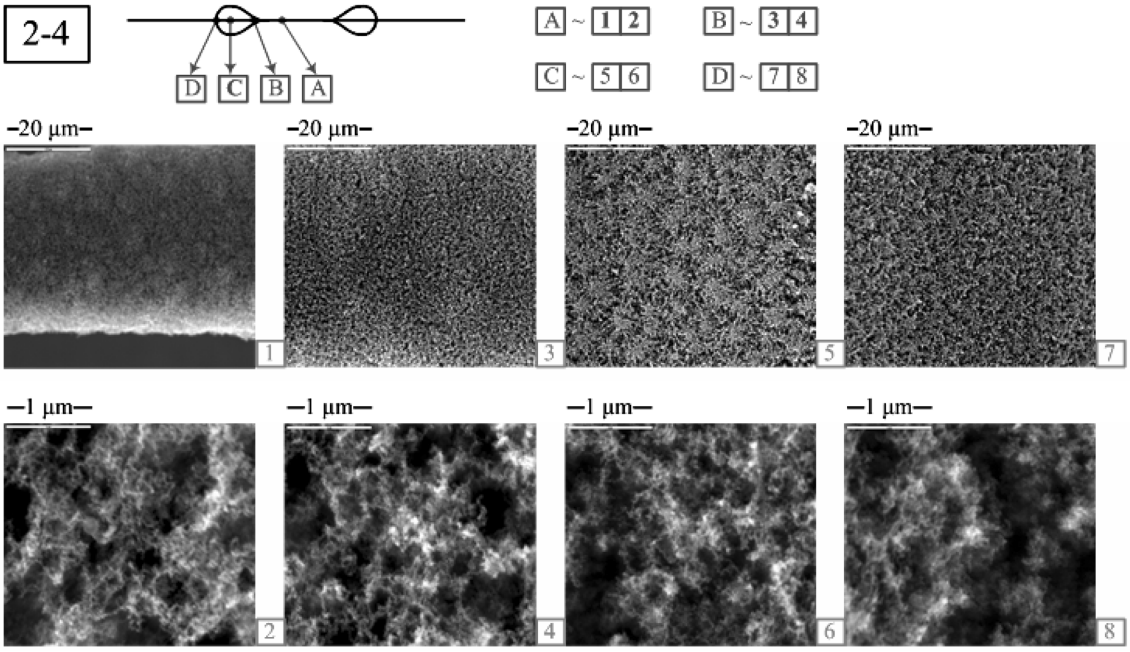

Fig. 6. Soot photographed at 2,000× (1-4) and 40,000× (5-8) by SEM. Sampled at the radial positions A, B, C and D in a methane-acetylene/air laminar diffusion flame. Nozzle ID=10 mm, Q_{fuel}=0.25 L/min with Q_{CH_4}=0.24 L/min and $Q_{C_2H_2}$=0.01 L/min, Q/Q_{sto}=2. Axial position: y=15 mm. The contour on the horizontal line represents deposits on the fiber.

cles are produced is represented. That is the transition from droplet-like deposits to individual soot particles. While from Fig. 6, because the axial position is lower than the position that the droplet-like phase is formed, another process is shown in which aggregation of the smaller soot particles occurs along the particle path lines. The addition of the acetylene in the methane laminar diffusion flame proved that C-C is important in the formation of the droplet-like phase and C=C is important in the formation of the PAHs and mature soot particles.

3. Cases 3 and 4

Fig. 7 shows deposits on SiC fibers captured in 2 minutes in a methane-acetylene/air co-flowing, laminar diffusion flame surrounded by co-flowing air. The fuel flow rate was 0.25 L/min with 0.15 L/min methane and 0.10 L/min acetylene, respectively. The co-flow-

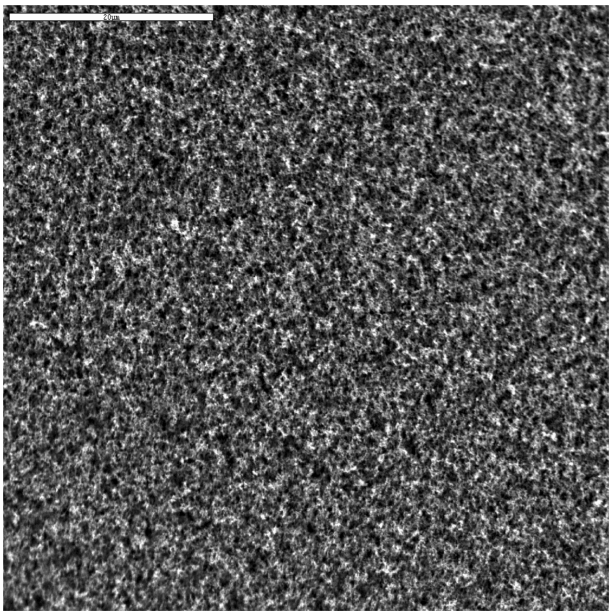

Fig. 7. Soot photographed at 2,000× SEM. Sampled in a methane-acetylene/air laminar diffusion flame. Nozzle ID=10 mm, Q_{fuel}=0.25 L/min with Q_{CH_4}=0.15 L/min and $Q_{C_2H_2}$=0.10 L/min, Q/Q_{sto}=2. Bar scale: 20 μm.

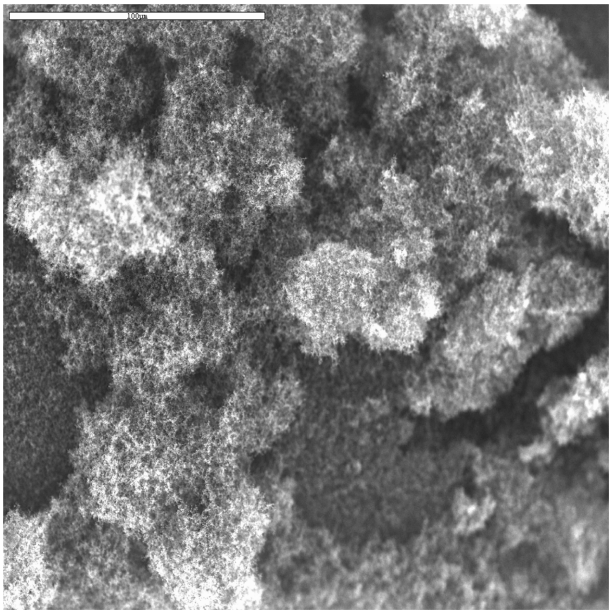

Fig. 8. Soot photographed at 2,000× SEM. Sampled from air. Bar scale: 100 μm.

ing air flow rate was still Q/Q_{sto}=2.

When the flow rates of acetylene were at 0.10 L/min and 0.25 L/min, the SEM deposit morphologies were both as in Fig. 7 with no radial and axial size difference on all fibers. Soot particles sizes were about 50 to 100 nm and not only on fibers but also formed floccules in air as shown in Fig. 8. The mature soot particles also did not become smaller by oxidation toward the radial end of the high temperature reaction zone and no distinct fiber-like structure was found because with abundant of C=C, soot particles form so fast even in low temperature reaction zone. It is concluded that the more acetylene that is added, which means more C=C is added, the more likely the process of smaller individual soot particles aggregation will occur.

CONCLUSIONS

In the present study, the morphologies of deposits on SiC fibers have been investigated by SEM in methane-acetylene/air co-flowing laminar diffusion flames.

Two kinds of processes by which mature soot particles are produced were proved to exist in flames: one is aggregated from the smaller soot particles, and the other is evolved from the condensed-phase deposits.

The results show that the size of the soot particles deposited in the luminous flame zone and the structures of the fiber-like formed outside the luminous flame zone are dependent on their axial and radial positions.

The addition of the acetylene in methane/air laminar diffusion flames proved that C-C is important in the formation of the droplet-like phase and C=C is important in the formation of the PAHs and mature soot particles. The more C=C that was added, the more likely the process of smaller individual soot particles aggregation would happen.

We are still studying different morphologies of deposits in flames with respect to fiber position, temperature, radical species and fuel species. Further studies are also to be performed in modeling, laser diagnostics and effect of electric field.

ACKNOWLEDGMENT

This work was supported by the National Key Basic Research and Development Program 2002CB211600. The SiC fibers used in the experiment were supplied by Mr. Sung Hoon Shim, Korea.

NOMENCLATURE

y : axial position of the fiber [mm]
X : magnification of SEM [times]
Q : gas flow rate [L/min]
Q_{sto} : stoichiometric flow rate [L/min]

REFERENCES

1. S. H. Shim and H. D. Shin, *Combustion and Flame*, **131**, 210 (2002).
2. S. H. Shim, K. Y. Ahn, S. H. Jeong, S. I. Keel and H. D. Shin, *Applied Energy*, **79**, 179 (2004).
3. M. Frenklach, S. Taki, M. B. Durgaprasad and R. A. Matula, *Combustion and Flame*, **54**, 81 (1983).
4. C. Bertrand and J. L. Delfau, *Combustion Science and Technology*, **44**, 29 (1985).
5. S. C. Rah, *Korean J. Chem. Eng.*, **2**, 1 (1985).
6. I. Glassman, *Twenty-second symposium, the combustion institute*, Pittsburgh, Pennsylvania, 295 (1988).
7. K. Saito, A. S. Gordon, F. A. Williams and W. F. Stickle, *Combustion Science and Technology*, **80**, 103 (1991).

8. R. Said, A. Garo and R. Borghi, *Combustion and Flame*, **108**, 71 (1997).
9. H. K. Choi, S. J. Park, J. H. Lim, S. D. Kim, H. S. Park and Y. O. Park, *Korean J. Chem. Eng.*, **19**, 342 (2002).
10. J. H. Choi, S. J. Ha and Y. O. Park, *Korean J. Chem. Eng.*, **19**, 711 (2002).
11. F. S. Liu, H. S. Guo, G. J. Smallwood and O. L. Gulder, *Combustion Theory Modeling*, **7**, 301 (2003).
12. H. J. Ryu, N. Y. Lim, D. H. Bae and G. T. Jin, *Korean J. Chem. Eng.*, **20**, 157 (2003).
13. K. C. Oh, U. D. Lee, H. D. Shin and E. J. Lee, *Combustion and Flame*, **140**, 249 (2005).
14. B. S. Haynes and H. G. Wagner, *Energy Combustion Science*, **7**, 229 (1981).
15. M. Frenklach, D. W. Clary, W. C. Gardiner Jr. and S. E. Stein, *Twenty-first symposium on combustion, the combustion institute*, Pittsburgh, Pennsylvania, 1067 (1986).
16. L. G. Blevins, M. W. Renfro, K. H. Lyle, N. M. Laurendeau and J. P. Gore, *Combustion and Flame*, **118**, 684 (1999).